A Critical Review on Sustainable Biochar System through Gasification: Energy and Environmental Applications

Siming You[1#], Yong Sik Ok[2#], Season S. Chen[3], Daniel C.W. Tsang[3], Eilhann E. Kwon[4], Jechan Lee[4], Chi-Hwa Wang[5*]

[1]*NUS Environmental Research Institute, National University of Singapore, Singapore 138602, Singapore;*

[2]*Korea Biochar Research Center, Kangwon National University, Chuncheon 24341, Korea;*

[3]*Department of Civil and Environmental Engineering, Hong Kong Polytechnic University, Hung Hom, Kowloon, Hong Kong, China;*

[4]*Department of Energy and Environment, Sejong University, Seoul 05006, Korea;*

[5]*Department of Chemical and Biomolecular Engineering, National University of Singapore, Singapore 117585, Singapore*

The authors contribute equally.

*Corresponding author: chewch@nus.edu.sg;

Abstract

This review lays great emphasis on production and characteristics of biochar through gasification. Specifically, the physicochemical properties and yield of biochar through the diverse gasification conditions associated with various types of biomass were extensively evaluated. In addition, potential application scenarios of biochar through gasification were explored and their environmental implications were discussed. To qualitatively evaluate biochar sustainability through the gasification process, all gasification products (*i.e.,* syngas and biochar) were evaluated via life cycle assessment (LCA). A concept of balancing syngas and biochar production for an economically and environmentally feasible gasification system was proposed and relevant challenges and solutions were suggested in this review.

Keywords: *Biochar; black carbon; pyrolysis; soil amendment; life cycle assessment.*

1. Introduction

Gasification can be defined as a thermochemical process which transfer heating value from carbonaceous materials into syngas (*i.e.*, a mixture of H_2 and CO), tars and biochar at high-temperature (>500 °C) and oxygen-deficient conditions. The gasification process generally involves four consecutive steps, *i.e.*, drying, pyrolysis (*i.e.*, thermally-induced fragmentation via bond dissociation and dehydrogenation), partial oxidation and reduction (Loha et al., 2014). In terms of the gas-solid contacting mode, gasifiers could be categorized into three major types: fixed bed, fluidized bed and entrained flow. In addition, their practical employments are highly contingent on the types of biomass and the compositional matrix of the final products.

In general, biochar yield from the gasification process is less than other thermochemical processes such as pyrolysis, which can be explicable by the conversion of carbon into carbon monoxide (CO) due to its partial oxidation conditions (Brewer et al., 2009; Mohan et al., 2014). Moreover, the operational conditions for gasification are varied to optimize a maximum energy (*i.e.*, syngas production) from the diverse carbonaceous feedstocks. The formation of biochar as a co-product of the gasification process is intentionally restricted to maximize the energy recovery (*i.e.*, the high yield of syngas). Indeed, this inevitably limits the operational parameters for the gasification process (Meyer et al., 2011).

Nevertheless, a great deal of researches conducted during the past decade envision fully enlightened the effectiveness of biochar as a principal strategy for carbon sequestration due to its recalcitrant properties. Therefore, the production of biochar from the gasification process possibly offers the wide-ranged operational conditions for the gasification process. In this context, most of the attention is focused on the soil amendment and carbon sequestration application of biochar which prefer a high biochar yield (Lehmann et al., 2011). However, this does not preclude the application potential of gasification biochar, and the economic and

environmental potential of gasification biochar systems could not be underestimated. Currently, a huge amount of biomass and waste are available for gasification, meaning a substantial amount of biochar will potentially be produced by gasification. In line with the constant development of new biochar modification methods, it is possible to fine-tune gasification biochar for diverse applications beyond soil amendment.

From a systemic perspective, producing biochar from the gasification process leads to several technical and economic merits. Firstly, gasification generally produces more energy per unit mass of carbonaceous material because of its high conversion efficiency of carbon compared to fast and slow pyrolysis and hydrothermal treatment (Hammond et al., 2011; Shackley et al., 2012a). Gasification featured by its autothermal nature (*i.e.*, exothermic reaction by the partial oxidation) provides self-sustaining energy support for reactions in a gasifier, thereby resulting in no use of inert gas like nitrogen and helium. Indeed, this significantly enhance the economic viability of the gasification process. Secondly, the electricity and heat production can potentially be used in feedstock-related upstream or biochar-related downstream treatment processes, which enhances the economic feasibility of the gasification system. For instance, the pretreatment (*e.g.*, drying and hydrolysis) of moist feedstock requires significant energy supply which can be obtained from the waste heat of the gasification system. Thirdly, the partial oxidizing environment during the gasification process may serve to improve the textural and chemical properties of gasification biochar which imparts the practical application of biochar (Manyà, 2012). Fourthly, gasification allows continuous feedstock feeding, which may cater to a higher throughput design than pyrolysis (Peterson & Jackson, 2014). Lastly, gasification is suitable for small- and medium-scale decentralized systems which have lower carbon conversion rates and thus higher biochar yields than large-scale systems (Shackley et al., 2012a).

This review focuses on (i) examining the physicochemical characteristics of gasification biochar; (ii) exploring feasible and non-soil applications of gasification biochar; (iii) discussing the role of biochar in gasification systems using life cycle assessment (LCA); (iv) addressing the identified economic, environmental, and technological challenges by a concept of balancing syngas and biochar production.

2. Gasification Biochar

2.1 Characteristics of gasification biochar

2.1.1 Physical properties

The pore volume and size, specific surface area and particle size of biochar are key parameters in defining the physical properties of biochar. The pore formation of biochar is closely related to the release of volatiles from polymeric backbone of carbonaceous feedstock (Chen et al., 2015). High volatile matter contents in the feedstock could promote the development of porous structures and the reactivity of biochar (Pacioni et al., 2016). Total pore volume is critical for the solid-gas interaction and exchange between gaseous reactants and the active sites on the surface of biochar (Sun et al., 2012). According to the classification of activated carbon pores by the International Union of Pure and Applied Chemistry (IUPAC), pores with diameter less than 2 nm, between 2 - 50 nm, and larger than 50 nm are grouped as micropores, mesopores, and macropores, respectively. The pore size determines the accessibility of the active sites and mass transfer limitation, and the surfaces of macropores and mesopores better represent the reactive surfaces compared to those of micropores (Wu et al., 2009). The specific surface area of biochar is defined as the ratio of the total pore surface area to the total

biochar particle mass, and it is well correlated with its porosity. The physical properties may affect the chemical properties of gasification biochar. For example, larger surface area and micropore volume have been found to be correlated with higher total polycyclic aromatic hydrocarbons (PAHs) on biochar surface (Rollinson, 2016). Alkali and alkaline earth metallic (AAEM) species (e.g., K, Na, Ca, Fe, and Mg) are commonly observed in biomass. These metallic species is known to have a crucial role in the gasification process for determining the variation of gasification products and the efficiency for gasification, which is likely due to the potential catalytic effects attributed by the common alkaline earth metallic species (Yip et al., 2009). Furthermore, the morphology of biochar can be affected by the dispersion of the AAEM species.

The specific surface area and pore volume of biochar are mainly influenced by the thermochemical conditions such as, temperature, residence time, and heating rate. The reported specific surface areas and total carbon contents of gasification biochar is shown in Figure 1. The specific surface area ranged from 14.3 to 748.5 $m^2 g^{-1}$. The carbon content was in the range from 21.8 to 89.9 wt.%. The specific surface area is generally positively related to the total carbon content, which could be well fitted by an exponential function, $y = 9.97e^{0.047x}$ (R^2=0.65). This suggests that the carbon material plays a critical role in building up the porous structures of gasification biochar. The switchgrass biochar generally had a low specific surface area (< 60 $m^2 g^{-1}$), while wood-related feedstocks gave higher surface areas and carbon contents. Hansen et al. (2015) attributed the higher specific surface area and pore volume for pine wood biochar than wheat straw biochar due to the higher process temperature required for wood. However, this difference in surface properties between the two biochar could also be resultant from the difference of feedstocks. A high mineral content in raw feedstocks may lower the specific

surface of gasification biochar by blocking the pores in the biochar (Hansen et al., 2015). The grape marc produced in a small-scale entrained flow gasifier had a low specific surface area (<70 g m^{-2}) which was attributed to the coalescence of smaller pores and the presence of fractures due to the thermal contractions and expansions as observed by SEM microscopy (Hernández et al., 2016). The red dash line denotes the lower bound of the specific surface area of activated carbon (500 $m^2 g^{-1}$) (Yeo et al., 2012). The specific surface area of gasification biochar is generally smaller than that of activated carbon, except for those with a total carbon content of around 80 wt.%

In general, gasification biochar had smaller specific surface areas and total pore volumes than those from slow and fast pyrolysis (Peterson & Jackson, 2014). This was mainly caused by the effects of ash melting (pore clogging), pore expansion and collapse, and tar deposition corresponding to the high temperatures during combustion and/or reduction stages of gasification. However, the gasification process using O_2 and steam as the gasifying reagents was similar to some physical activation processes that are used to produce activated carbons with high specific surface areas and total pore volume (Manyà, 2012; Xiu et al., 2017). Due to the activation effect of the gasifying agents, the decrease in the specific surface area and total pore volume may be partly offset. After the activation process, the surface area and total pore volume could increase by up to one order-of-magnitude (Bhandari et al., 2014) and the surface areas (800 - 900 $m^2 g^{-1}$) of the resulting activated carbons are comparable to or even larger than those from of pyrolysis biochar (Angın et al., 2013; Zhang et al., 2014). Brewer et al. (2011) showed that the specific surface area of gasification biochar under the gasifying agent of O_2 or steam could be double of that of pyrolysis biochar for the same feedstocks.

147 The significantly shorter residence time of gasification (seconds) than that of slow pyrolysis
148 (hours to days) leads to rapid devolatilization in the feedstock and hence results in smaller
149 particle sizes in the former (Brewer et al., 2009; Scala et al., 2006). The biochar size distribution
150 depends on the types of biomass and thermochemical conditions (*e.g.*, temperature and gasifying
151 agent) (Cetin et al., 2004). The particle sizes of gasification biochar ranged from less than 45 μm
152 to more than 2000 μm and it lacks consistency among the findings of existing studies (Griffith et
153 al., 2013; Hansen et al., 2015; Ojeda et al., 2015; Pereira et al., 2016; Shen et al., 2016b).
154

155 **2.1.2 Chemical properties**

156 The chemical properties that are potentially relevant to biochar applications include carbon
157 and ash contents, AAEM species, functional groups, aromaticity, and pH. The composition and
158 reactivity of biochar are closely related to the thermochemical production conditions (*e.g.*,
159 temperature, gasifying agent, and equivalence ratio) and the types of biomass (Naisse et al., 2013;
160 Spokas et al., 2011).

161 The total carbon, ash and inorganic elements in gasification biochar are summarized in Table
162 1. The ash content in gasification biochar can be reached up to 60 wt.% and is generally higher
163 than their raw feedstock because of the loss of volatile matters and the enrichment of inorganic
164 components. The concentrations of inorganic elements in gasification biochar could be up to
165 1500 times higher than those in their raw feedstocks (Shen et al., 2016). During the gasification
166 of sewage sludge in an updraft fixed bed gasifier, most of the elements were enriched by three
167 times in the ash compared to the raw sludge while particle evaporation occurred at high
168 temperatures for some volatile elements such as Pb and Zn, leading to the reduction in their
169 concentrations (Kim et al., 2016). Inorganic compositions are expected to be conserved only if
170 the process temperature is lower than their respective volatilization temperature. If the process

temperature in a gasifier exceeds the melting point of certain metals (e.g., Zn, Cd, As, Se, K, and Na), these metals/metalloids could be volatilized and have low concentrations in the biochar (Shackley et al., 2012b). An over-high alkali content in the initial feedstock and thus gasification biochar may lower the melting temperature of ash, which cause ash agglomeration, slagging, and fouling problems (Hernández et al., 2016). Ash agglomeration occurred when the peak temperature at the ignition front was above the initial deformation temperature of ash with a low combustion rate and an increased stoichiometry (Kim et al., 2016).

The carbon content of gasification biochar was previously suggested to be in the range of 20 - 60 wt.%, which was generally smaller than that of pyrolysis biochar (50 - 80 wt.%) (Yu et al., 2009). This was attributed to the fact that a relatively high temperature (>500 °C) and the presence of limited amount of oxygen in a gasifier serve to oxidize carbon into CO_2. However, Table 1 showed that the total carbon content of gasification biochar could be well over 60 wt. %. Although gasification biochar generally contains a lesser amount of carbon, it presents more condensed aromatic rings (~ 17 rings per compound) (Brewer et al., 2009; Sohi et al., 2010). The highly condensed structure of biochar is attributed to the high reaction temperature during the gasification process (Brewer et al., 2009). As a result, gasification biochar shows more resistance to chemical oxidation and microbial mineralization, which may increase the difficulty in the modification of their surface functionality (Marks et al., 2016). The relatively high temperature and the existence of a partial oxidation stage also cause gasification biochar to have a higher ash content and pH value than pyrolysis biochar (Enders et al., 2012; Marks et al., 2016; Peterson & Jackson, 2014). The ash content of gasification biochar should also depend on the types of feedstocks. For example, the gasification biochar from corn stover have a significantly higher ash and inorganic elements than those from oak (Cheah et al., 2014). Gasification of grape marc

194 in a small-scale entrained flow gasifier showed that approximately 70-80 wt.% of inorganic
195 elements were retained in the biochar, and the fraction decreased at higher temperatures
196 (Hernández et al., 2016).

197 Phenol, ether, quinone and pyrone were found to be the dominant O-containing functions on
198 the surface of wood chip gasification biochar (Ducousso et al., 2015). The oxygenated surface
199 functional groups are referred to as acidic surface groups and are normally formed by the
200 reactions at a temperature between 200 and 700 ˚C (Rogovska et al., 2012). The acidic surface
201 groups are generally unstable and affect the reactivity of gasification biochar upon their
202 application as catalysts. Basic and neutral surface functional groups are relatively stable and are
203 formed at lower temperatures. Oxygen chemisorption (oxygenation by an O_2 gas-phase treatment)
204 has been applied to increase the O-containing functionality on biochar surfaces (Ducousso et al.,
205 2015). After oxygenation, the content of hydroxyl, peroxides, lactones, and anhydrides
206 functional groups significantly increased, with hydroxyl being particularly favored by high
207 temperatures.

208 However, the high temperature in a gasifier could cause a significant loss of functional
209 groups such as hydroxyl, carboxyl, and carbonyl. As a result, gasification biochar generally
210 poses less functional groups than the biochar produced from the other thermochemical processes
211 such as pyrolysis and hydrothermal carbonization (Wiedner et al., 2013). Specifically,
212 gasification biochar was found to have a smaller fraction (~10 wt.%) of aromatic C-H groups
213 than the biochar from slow (~30 wt.%) and fast (~23 wt.%) pyrolysis (Brewer et al., 2011). This
214 difference suggests that the application capacity and potential of gasification biochar may differ
215 from pyrolysis biochar since the surface functionalities of carbon materials are directly related to

their physicochemical and electrochemical properties such as wettability, electrical conductivity, capacitance, pH, point of zero charge, and self-discharge characteristics (Rabou et al., 2009).

Corresponding to the lower density of functional groups, gasification biochar generally had a higher degree of aromaticity (the fraction of carbons in biochar that form aromatic rings) than pyrolysis biochar (Abdulrazzaq et al., 2014). A high degree of aromaticity suggests a low content of readily degradable compounds and a highly condensed carbon structure with a strong resistance to chemical oxidation (Hardy & Dufey, 2017). Hence, the aromaticity and degree of aromatic condensation of biochar play an important role in determining the stability or persistence of biochar in the environment (Wiedemeier et al., 2015). The degree of aromaticity of biochar could be evaluated using van Krevelen diagrams by plotting the molar ratio H/C against O/C. A small H/C or O/C ratio means that the biochar consists predominantly of fixed carbon aromatic rings and thus is chemically stable. The van Krevelen diagram for the gasification biochar reported in existing literature is shown in Figure 2.

The red dash lines denote the recommended upper bound limits (0.6 and 0.4, respectively) of H/C and O/C ratios for biochar materials by European Biochar Certificate (EBC). The gasification biochar generally has the ratios well within the limits, except for the study by Plácido & Capareda (2015) which had an H/C ratio around 1. This should be related to the relatively low temperatures (500 - 600 °C) applied in the gasification processes, which mitigated the decomposition of hydrogen functional groups in the biochar. The aromaticity of biochar would increase as temperature increased (McBeath et al., 2011; Wiedemeier et al., 2015). Increasing the process temperature would enhance the carbonization degree of biochar, leading to the decrease of H/C and O/C ratios and amorphous organic matters (Beesley et al., 2011; Spokas, 2010). An extremely low O/C ratio may suggest a minimal polarity and high

hydrophobicity of biochar which was found in the sewage sludge, bluegrass seed screenings, and white oak biochar, and this may enhance the biochar's performance in CO_2 capture in the presence of water (Shen et al., 2016).

The pH values of gasification biochar generally fall into the alkaline range (7<pH<12) (Hansen et al., 2016b; Shackley et al., 2012b; Wiedner et al., 2013). This should be directly related to their metal salt and/or ash content and high degree of carbonization (Griffith et al., 2013; Shen et al., 2016). For example, and the highest pH values of gasification biochar corresponded to the highest elemental fractions of metals such as K and P (Yargicoglu et al., 2015). In contrast, the biochar from hydrothermal carbonization, fast pyrolysis, and slow pyrolysis were acidic, near neutral pH values, and ranging from acidic to alkaline, respectively (Yu et al., 2009).

2.1.3 Biochar yield

The variation of gasification biochar yield with respect to temperature (550 - 1350 °C), the types of gasifiers and feedstocks, and gasifying agents is given in Figure 3. The red dash lines denote the biochar yield based on pyrolysis (Manyà, 2012). Biochar yield through gasification was generally smaller than 200 g kg^{-1} for poplar wood, almond shell, pine wood, wheat straw, poultry litter, eucalyptus, pyrolysis oil, grape marc, miscanthus, switchgrass, and maize cobs, compared to 200 - 500 g kg^{-1} for biochar yield through pyrolysis. However, sewage sludge (Kim et al., 2016), rice husk (Shackley et al., 2012b), and waste tire (Xiao et al., 2008) biochar were three obvious exceptions with relatively high yields. For the sewage sludge and rice husk biochar, the high yields were related to the high ash contents in the original feedstocks, i.e. up to 36 and 24% for sewage sludge and rice husk, respectively The waste tire (a mixture of polymer and

carbon black) had a high carbon content over 80 wt.%. Under the relatively low temperature of 400 - 800 ˚C, most of the polymer was evaporated as volatile matter and the residual mass after gasification was roughly equivalent to that from the pyrolysis process. For the same type of feedstock, the gasification biochar yield generally decreases as the temperature increases. Corresponding to their high temperatures, the biochar yields from industry-scale entrained flow gasifiers were generally low. Leijenhorst et al. (2015) gasified pine wood- and wheat straw-derived pyrolysis oil at 1200 - 1500 °C in an entrained flow gasifier with a thermal throughput of 1 MW. The resultant biochar productions were 0.8 and 0.7 wt.%, for pine wood- and wheat straw- derived pyrolysis oil, respectively.

2.2. Applications of gasification biochar beyond soil amendment

2.2.1 Gasification biochar for tar removal

The generation of tars during the biomass gasification is harmful to the system, which could cause mechanical breakdown and deactivate the catalysts in the refining process (Shen, 2015). The aromatic compounds such as benzene and PAHs in tars also pose environmental hazards (Guan et al., 2012). Thermal and catalytic cracking techniques are available for tar removal (Han & Kim, 2008). Biochar are recently employed as catalysts to decompose tar. The relatively high surface area and porous structure of biochar could improve the dispersion of metal ions and facilitate the transport of reactant molecules into the internal surfaces of catalysts, which make them good catalyst supports (Shen & Yoshikawa, 2013). The major mechanisms of tar removal by biochar-based catalysts are physical adsorption, thermochemical reforming, and a combination of adsorption and catalytic conversion (Shen, 2015).

The removal capability of gasification biochar as a catalyst toward some model tars (phenol and naphthalene) has been shown to be comparable with that of commonly used catalysts such as calcined dolomite, olivine, and commercial nickel catalyst (El-Rub et al., 2008). However, the commercial catalysts are much more expensive and are easily deactivated by carbon fouling (e.g., coke deposition on nickel-based catalysts), and product gas contamination (Chan & Tanksale, 2014).

The gasification biochar achieved over 80 and 90% of phenol and naphthalene conversion under a temperature from 700 to 900 ˚C, respectively, of which the conversion efficiency increased with elevating temperature (El-Rub et al., 2008). Considering the continuous production of biochar from the gasification process, El-Rub et al. (2008) argued that the gasification biochar served as a good candidate catalyst for stable tar removal. Lower carbon content in the biochar may lead to lower tar removal, as other constituents in the biochar such as ash are ineffective for tar removal (Bhandari et al., 2014). The catalytic performance of biochar may be further improved by attaching active metal such as nickel to the surface of biochar. In the study by Qian & Kumar (2015), the red cedar char from a downdraft gasifier was activated by KOH under a nitrogen flow and impregnated with nickel nitrate solution followed by drying and reduction in a hydrogen flow for 3 h. The obtained catalyst was applied to remove lignin tar. The reaction temperature had a positive effect on the removal efficiency of most of the tar components except naphthalene. As pressure increased from 0.1 to 1.1 MPa, the removal efficiencies of most of the aromatic hydrocarbons and phenols increased from 0 to 70% and from 30 to 70%, respectively. This biochar-derived catalyst also achieved nearly 100 % removal for catechol, 2-methoxyvinylphenol, 4-methylcatechol, and o-xylene at 1.1 MPa.

306 The surface area and pore radius and volume of biochar-derived or activated carbon (from
307 biochar)-derived catalysts decreased significantly after tar removal experiments, suggesting that
308 it is critical to regenerate the catalysts for their commercialization. For example, the pore volume
309 of gasification biochar-derived catalysts decreased by 88 % after usage, which should be related
310 to the deposition of graphitic carbon on the catalysts leading to a coking effect, i.e., blockage of
311 pores (Bhandari et al., 2014). This means the deactivation of catalysts over time and a negative
312 relationship between tar removal efficiency and time on stream. Potential problems for biochar
313 with respect to their catalyst application include (1) degradation of surface properties of biochar
314 and (2) variability in catalytic performance due to coking effect (Bhandari et al., 2014). However,
315 some studies (Fortier et al., 2008; Xu et al., 2009) suggested that the neutral or weak base
316 properties of gasification biochar may enhance the catalyst's resistance to deactivation due to
317 carbon and metal deposition. Meanwhile, the carbon deposition and thus coke formation can be
318 reduced by the effective use of catalyst supports such as dolomite and MgO and the addition of
319 AAEM species which are commonly found in raw gasification biochar. Basic supports are
320 generally more coke-resistant than acidic supports (Chan & Tanksale, 2014). For example, metal
321 elements such as Pt, Co and Cu could serve as promoters to improve the catalytic activity of
322 nickel-based catalysts by enhancing (1) nickel reducibility by forming strong interaction with
323 nickel, (2) dispersion of nickel on the support, and (3) resistance to coke formation (Chan &
324 Tanksale, 2014).
325

326 **2.2.2 Gasification biochar as fuel**

327 Biochar produced from gasification can be recycled back to the gasification process as fuel,
328 as such biochar contains high carbon content and calorific value. Due to their high heating values,

329 gasification biochar could be used as the feedstock of gasification to convert the residual carbon
330 "left" in a previous gasification process to extra gaseous fuel (Le & Kolaczkowski, 2015; Pacioni
331 et al., 2016). In that sense, they are often referred to as charcoal. For example, the palm kernel
332 shell biochar from a bubbling gasifier exhibited 75-91 % carbon content with a high heating
333 value of around 28 MJ kg^{-1}, which was comparable to the heating values of bituminous coal
334 (Bazargan et al., 2014). Note that the skeletal density of biochar was in the range of 1340 - 1960
335 kg m^{-3} (Brewer et al., 2014) which is slightly higher than bituminous coal (1250 - 1350 kg m^{-3})
336 (Zhao et al., 2015). The reactivity of biochar is related to the carbon conversion levels upon its
337 production, which further depends on the types of feedstocks. Negative relationships were found
338 for the biochar of refuse derived fuel and coal (Le & Kolaczkowski, 2015; Liu et al., 2006),
339 while a positive relationship was found for wood biochar (Mermoud et al., 2006). The mineral
340 composition in feedstocks strongly affected the reactivity of gasification. Especially, the AAEM
341 species in gasification biochar may serve as catalysts to promote the gasification process (Wu et
342 al., 2009). For example, higher K and Ca contents in the biochar of spent coffee grounds and
343 apple pomace led to a significant higher gasification reaction rate compared to the biochar of
344 sawdust because of the catalytic effect of mineral elements (Pacioni et al., 2016). Compared to
345 the biochar with AAEM species being removed by acid treatment, the raw biochar showed a
346 higher reactivity (Yip et al., 2009). Ma et al. (2016) further showed that the AAEM species had a
347 significant effect on the water gas shift reaction ($CO\ (g) + H_2O\ (g) \leftrightarrow CO_2\ (g) + H_2\ (g)$) during
348 the catalytic steam reforming of bio-oil model compounds. The presence of Na, K, and Ca
349 exhibited the strongest catalytic effect for biochar gasification (Dupont et al., 2011; Yip et al.,
350 2009). Nevertheless, excessive ash content in gasification biochar possibly leads to the
351 encapsulation of AAEM species and a reduced porosity, hence, adversely affecting the reactivity

of biochar. The presence of tar in biochar could inhibit the gasification reactions when gasification biochar are used as the feedstock (Nzihou et al., 2013).

2.2.3 Gasification biochar as adsorbent

Gasification biochar with high surface areas, pore volume, and oxygen-containing surface functional groups could be directly used as adsorbents to remove heavy metals and/or organic pollutants in the environment (Prasara-A & Gheewala, 2016; Thompson et al., 2016). The adsorption capacity should be mainly related to the physical properties of biochar. Improvement in pore structure such as enlarged pore sizes and a higher density of functional groups could enhance the adsorption capacity of biochar for methylene and heavy metals, respectively (Rafatullah et al., 2010; Wang et al., 2013). An increase in the specific surface area of biochar was associated with a higher sorption capacity for organic chemicals, such as pesticides and herbicides (Kasozi et al., 2010; Yu et al., 2015). The presence of oxygen-rich functional groups such as C-O and C=O, and aromatic groups on gasification biochar could serve as strong active sites and enhance biochar's adsorption capability (Xue et al., 2012).

Gasification biochar could also serve as the precursor of activated carbon featured by a larger porosity and specific surface area, and thus greater adsorption capability (Qian et al., 2015). The physical activation method involves the use of the gases such as steam, CO_2, or ozone under a temperature higher than 700 ˚C, while chemical agents such as KOH, NaOH, NH_3, and $ZnCl_2$ are used in the chemical activation methods. Activation significantly increases the specific surface area and pore fraction of original biochar and benefit the downstream applications of activated carbon as adsorbents (Angın et al., 2013). Bhandari et al. (2014) converted switchgrass gasification biochar into activated carbon by ultrasonic impregnation of

potassium hydroxide (KOH) and found that introducing ultrasonication to the activation process of the biochar from the downdraft gasifier could significantly increase the specific surface area of the resulting activated carbon. The specific surface areas and total pore volume of the resulting activated carbon were 150 and 50 times of original biochar. The authors also showed that the original biochar contained un-burnt biomass particles and some biochar particles were closed and non-porous. After activation, however, clear porous structures were created by the volatilization and wash-out of solid residues by thermal treatment and wash cycles during activation.

Activating agents could also affect the properties of activated carbon. Tay et al. (2009) showed that K_2CO_3 was a more effective agent than KOH in activating soybean oil cake biochar, and it could produce the activated carbon of a higher porosity, larger yield, and less ash and sulfur contents. Zhang et al. (2014) found that CO_2-activated biochar had a higher CO_2 adsorption capacity than NH_3- and CO_2-NH_3-activated biochar at a temperature of 20 °C. At a temperature of 120 °C, the adsorption capacity depended on the N-content of biochar and the CO_2-NH_3-activated biochar had the highest CO_2 adsorption capacity due to the formation of nitrogen functional groups from the reaction between biochar carbon and ammonia. The activated carbon from switchgrass gasification biochar showed an effective toluene removal rate of 69-92% (Bhandari et al., 2014). Maneerung et al. (2016) activated the wood gasification biochar via steam, which showed a high adsorption capability (189.83 mg g^{-1}) towards Rhodamine B.

2.2.4 Gasification biochar for electrochemical applications

Direct carbon fuel cells (DCFCs) have been received increasing attention due to their greater electrical efficiency, size flexibility, and overall reliability, compared with conventional technologies such as steam and gas turbines (Giddey et al., 2012). The high carbon content and carbon-oxygen groups in biochar facilitate their application as the carbon material in DCFCs to generate a high amount of valuable gases (CO, H_2, and CH_4) (Elleuch et al., 2015). A DCFC system based on wood biochar achieved a power density level around 60 - 70 % of that based on coal (Ahn et al., 2013b). The carbon content, specific surface area, and total pore volume of biochar determine the performance of a biochar-based DCFC system by affecting the electrochemical reactions, which are positively related to the maximum power density of a DCFC system (Ahn et al., 2013a). High specific surface area and total pore volume facilitate the reactivity of the anode electrochemical reaction and lead to a higher maximum power density in a DCFC system (Ahn et al., 2013a; Ahn et al., 2013b). The reactivity and specific surface area of biochar may play a complementary role to each other to affect the performance of a biochar-based DCFC. For example, although the specific surface area (244.6 m^2 g^{-1}) of corn stover biochar was smaller than that (750 m^2 g^{-1}) of activated carbon, its high reactivity (the lost rate of biochar mass) helped to achieve highly effective char utilization and support current loads surpassing 500 mA cm^{-2} (Alexander et al., 2012). One of the potential technical demerits associated with the fuel cell performance was reported as cell degradation (Munnings et al., 2014). This degradation is effected by two main factors: (1) less and less fuel is available for reactions upon the consumption of carbon materials and (2) after carbon consumption, more and more ash gets in contact with the anode, which further reduces the reaction surface area and

418 blocks the charge transfer through the cell. Hence, the ash content of gasification biochar needs
419 to be paid special attention when they were applied in a DCFC system.

420 The properties of high electrical conductivity, thermal and chemical stability, and large
421 specific surface area of gasification biochar suggest their great potential for other
422 electrochemistry-related applications such as electrocatalyst and supercapacitors. For example,
423 pine wood gasification biochar have been used as cathode electrocatalyst supports (Huggins et al.,
424 2015). The original biochar were first sonicated for 30-min followed by 2-h heating in a 3 M
425 KOH aqueous solution. The treated biochar were then used as a manganese oxide electrocatalytic
426 support for microbial fuel cells (MFCs). The electrocatalyst support achieved satisfactory
427 maximum power densities which were comparable to the ones based on the conventional, more
428 (50 %) expensive cathode material, Vulcan Carbon (VC). Small-scale tests in single-chamber
429 MFCs inoculated with anaerobic sludge suggested that the gasification biochar could be used as
430 an effective, economical, and scalable electrocatalyst for MFC application.

431 The gasification biochar from a mixture of biomass and polymeric waste has been upgraded
432 into carbon nano-tubes which have high electronic conductivities and specific surface areas and
433 could potentially serve as an electrocatalyst support for fuel cells and electrode materials of
434 lithium-ion batteries (Esfahani et al., 2017). It is worth noting that pre-processing activities such
435 as sieving and milling may be needed to achieve the uniformity of biochar particle sizes for good
436 electrochemical performance. Biochar have also been used as the electrode materials of
437 supercapacitors because of their potentially high electrical conductivity and high electrochemical
438 activity (Chen et al., 2015; Li et al., 2017). Under a high reaction temperature of 1200 °C, the
439 electrical conductivities of gasification biochar of poplar wood, wheat straw, wood chips,
440 sorghum, and olive residues were found to be 997, 1327, 288, 502, and 238 μS cm^{-1}, respectively

441 (Wiedner et al., 2013). The capacitive performance of biochar-based supercapacitors is
442 influenced by the specific surface area, pore structure and distribution, electrical conductivity
443 and surface functionalities of biochar (Abioye & Ani, 2015).

444 In general, the electrochemical performance of biochar should be related to its texture and
445 surface chemistry, especially, the concentration of O-containing functional groups (Li et al.,
446 2009). The conductive properties of biochar were found to be positively related to its degree of
447 aromaticity, i.e. its fused-ring aromatic structures and anomeric O-C-O carbons (Li et al., 2013).
448 The functional groups on biochar correspond to the presence of heteroatoms such as oxygen,
449 nitrogen, and sulfur which are closely associated with biochar's surface chemical heterogeneity.
450 These heteroatoms originate from raw feedstocks and are integrated into the carbon matrix due to
451 incomplete carbonization (Shafeeyan et al., 2010). In recent, the electrical conductivity of
452 biochar was found to be closely associated with its degree of carbonization (Gabhi et al., 2017),
453 where a six-order magnitude increase was observed as the carbon content of biochar increased
454 from 86.8 to 93.7 wt%.

455

456 **2.2.5 Gasification biochar as additives for anaerobic digestion (AD)**

457 Gasification-derived pine wood and white oak biochar have been used as additives for the
458 mesophilic and thermophilic AD of wastewater sludge to enhance methanogenic microbial-
459 activities and reduce the CO_2 content in biogas (Shen et al., 2016). The resulting methane content
460 in biogas was up to 92.3 and 79.0 vol.%, while 66.2 and 32.4 vol.% of CO_2 was sequestered
461 during the mesophilic and thermophilic AD, respectively. The biogas from an ordinary AD
462 process of sludge generally consists of 50-70 and 30-50 vol.% of methane and CO_2, respectively
463 (Appels et al., 2008). The biochar also enriched the macro- and micronutrients (*i.e.*, K, Ca, Mg,

464 and Fe) in the digestate and made it suitable as a fertilizer (Shen et al., 2016). The AAEM
465 species contained in the gasification biochar could be released in the form of cations which may
466 react with CO_2 from AD to generate HCO_3^-/CO_3^{2-} buffer. As a result, the pH of the digester
467 increased with the addition of gasification biochar and maintained in an alkaline range (7.23-7.43
468 and 7.43-7.61 for mesophilic and thermophilic, respectively) throughout the mesophilic and
469 thermophilic AD processes. This alkaline pH range led to an increase in the stability of
470 mesophilic AD. Because of the high degree of aromaticity of gasification biochar, the biochar-
471 amended AD showed a remarkably higher electrical conductivity than AD without biochar. It
472 was speculated that conductive biochar could promote the direct interspecies electron transfer
473 between syntrophic acetogen and methanogen communities by serving as an electron conductor
474 in an AD process, thus, accelerating methanogenesis (Shen et al., 2016). Furthermore, the large
475 specific surface area and porous structure of biochar favor the colonization of syntrophic
476 acetogenic bacteria and methanogenic archaea, which together with the increased reaction rate
477 facilitated the total organic carbon removal by AD (Cetin et al., 2004; Luo et al., 2015).
478

479 **2.2.6 Gasification biochar as catalyst for biodiesel production**

480 Biodiesel, a mixture of methyl esters, has the advantages of carbon neutrality, bio-
481 degradability, and low CO and particulate matter emission for automobile application. Lee et al.
482 (2017) investigated the non-catalytic transesterification of olive oil by using the maize residue
483 biochar from pyrolysis and dimethyl carbonate (DMC) as an acyl acceptor. They achieved a
484 biodiesel yield to 95.4% under the optimal operational conditions (380 °C and molar ratio of
485 DMC to olive oil (36:1)). The maize residue biochar from pyrolysis was used as porous media
486 for the thermally-induced non-catalytic transesterification reaction to synthesize fatty acid ethyl

esters (FAEE) from coconut oil (Jung et al., 2017). The wide pore distribution in the biochar was shown to enhance the yield of FAEEs, resulting in 87% yield of FAEE at 380 °C. In recent, the performance of the gasification biochar from palm kernel shells as a CaO (quicklime/burnt lime) catalyst for biodiesel production has been examined (Bazargan et al., 2015). The biochar had a high calcium content, mainly in the form of $CaCO_3$. The gasification biochar-based CaO catalyst had the advantage of low synthesis temperature and showed a satisfactory catalytic effect on the transesterification of sunflower oil with methanol (1:9). The reaction could be accelerated upon the increase in the loading of catalyst. The results showed that $CaCO_3$ contained in the palm kernel shell biochar was a promising low-cost source for CaO catalyst production. The thermal decomposition temperature (750 ˚C) of $CaCO_3$ to CaO in the biochar was found to be lower than that (> 900 °C) of raw limestone calcination, which was attributed to certain functional groups in the biomass that led to distorted crystal morphology and consequently lowered apparent activation energy for calcite decomposition (Thompson et al., 2014). Pyrolysis biochar-based studies (Dehkhoda et al., 2010; Kastner et al., 2012) suggested that a larger specific surface area and higher acid density of the catalyst were related to a higher biodiesel yield. Hence, the alkaline nature of gasification biochar may adversely affect its application for biodiesel production, which requires further investigation for improvement

3. Life cycle assessment (LCA) and Future Challenges

3.1 LCA

The potential economic and environmental (carbon abatement) benefits associated with the deployment of a gasification system could be judged by LCA. Biochar proved to be able to sequester carbon in the form of biochar with high persistence in soil environments. The findings

of the advantages of applying biochar for agricultural purpose stimulate wide consideration of the carbon sequestration effect of biochar in LCA (Ibarrola et al., 2012; Nguyen et al., 2013). A typical system boundary of LCA for a gasification-based waste disposal scheme without considering the waste generation process is shown in Figure 4.

Since the main product from gasification is syngas, the energy offset by displacing conventional fossil fuels (*e.g.*, coal, oil, and natural gas) generally plays a dominant role in the system's overall carbon abatement capacity followed by the carbon sequestration and soil effects by biochar, respectively (Ibarrola et al., 2012). The energy production by walnut shell gasification used to displace grid electricity could account for 91.8 %, and the carbon sink role of biochar accounted for 8.2 % of the total carbon abatement (Pereira et al., 2016). In contrast, the energy production from a pyrolysis system accounted for 10 – 25 % of the overall carbon abatement while the biochar-related carbon abatement contributed to 40 - 66% of the overall carbon abatement due to its high biochar yield (Elmouwahidi et al., 2012).

Consistently, Hammond et al. (2011) showed that gasification systems generally offer a lower carbon abatement potential than pyrolysis systems where the carbon stored in biochar would generally account for the greatest carbon abatement portion among all the carbon abatement components. The authors showed that gasification systems tend to produce more electricity than pyrolysis system, suggesting the economic advantage of gasification. Nguyen et al. (2013) found that the electricity production from the gasification of straw was more environmentally friendly than direct combustion because of: (1) a higher electricity generation efficiency, (2) a lower exhaust emission, and (3) biochar generation. Most of the previous LCA studies considered the application of biochar as a soil amendment. Relevant LCA considering the

applications of gasification biochar beyond soil amendment (Section 2.2) is still limited and needs to be explored in the future.

3.2 Challenges and perspectives

Upon the design of a gasification system, engineers and researchers often face up to a dilemma on balancing between the carbon abatement potential and overall energy delivery, which is further tangled by considering the potential applications of gasification biochar. It is more economically viable to produce more electricity because of its higher profitability compared to biochar for the time being (Meyer et al., 2011). However, this situation may change as the constant development of new biochar applications and the increasing demand of gasification biochar. The most environmentally or economically sustainable gasification system will achieve a balance between energy output and biochar generation, under which we need to consider: (1) the source of gasification feedstock (waste or biomass), (2) the syngas yield, composition, and applications (3) biochar yield and its physicochemical properties and applications, and (4) the respective carbon abatement potential of applying syngas as a renewable energy and applying biochar as a renewable source. A schematic of this concept is shown in Figure 5. In the future, it is worth exploring novel and unconventional biochar application scenarios and using LCA to optimize the combined economic and environmental performance of gasification systems.

To achieve robust engineering design and development of sustainable gasification systems, the capability of developing bespoke biochar is a must, that is, for a particular application, we need to know how much specific surface area, pore volume, carbon content, specific functional groups, etc, are desirable and what kind of gasification conditions are required to produce the

555 corresponding physicochemical properties. Hence, it is critical to understand the influences of
556 feedstock and thermochemical conditions towards the properties and performance of gasification
557 biochar. This is especially an urgent demand for gasification biochar because their relevant
558 studies are far less than other types of biochar mismatching their great application potential in
559 the industry. Specifically, a complete report of experimental conditions (gasifying agent,
560 temperature, feedstock, gasifier types) is needed to facilitate inter-study comparisons. Finally, a
561 thorough toxicology assessment is also needed prior to the practical application of gasification
562 biochar. The current assessment methods and the guideline values of contaminants (e.g., 12 μg g^{-1}
563 for 16 US EPA PAHs according to European Biochar Certificate guidelines) are mainly based
564 on the soil application of biochar which need to be extended to cater for the increasing
565 applications of biochar beyond soil amendment.
566

567 ## 4. Conclusions

568 The production, physicochemical properties and yield of gasification biochar are extensively
569 reviewed. Biochar from gasification have found their applications in removing tars, serving as
570 gasification feedstock and a precursor as activated carbon, adsorbing contaminants, DCFC,
571 amending AD, catalyzing biodiesel production, and being upgraded to oxygenated catalyst, with
572 satisfactory performance. Complete experimental conditions (gasifying agent, temperature,
573 feedstock, gasifier types) should be reported to facilitate between-study comparisons. A concept
574 of balancing syngas and biochar production for an economically and environmentally feasible
575 gasification system was proposed.
576

Acknowledgement

Chi-Hwa Wang and Siming You acknowledge the funding support by the National Research Foundation (NRF), Prime Minister's Office, Singapore under its Campus for Research Excellence and Technological Enterprise (CREATE) program. Grant Number R-706-001-101-281, National University of Singapore.

References

Abdulrazzaq, H., Jol, H., Husni, A., Abu-Bakr, R. 2014. Characterization and stabilisation of biochar obtained from empty fruit bunch, wood, and rice husk. *BioResources*, **9**(2), 2888-2898.

Abioye, A.M., Ani, F.N. 2015. Recent development in the production of activated carbon electrodes from agricultural waste biomass for supercapacitors: A review. *Renew. Sustainable Energy Rev.*, **52**, 1282-1293.

Ahn, S.Y., Eom, S.Y., Rhie, Y.H., Sung, Y.M., Moon, C.E., Choi, G.M., Kim, D.J. 2013a. Application of refuse fuels in a direct carbon fuel cell system. *Energy*, **51**, 447-456.

Ahn, S.Y., Eom, S.Y., Rhie, Y.H., Sung, Y.M., Moon, C.E., Choi, G.M., Kim, D.J. 2013b. Utilization of wood biomass char in a direct carbon fuel cell (DCFC) system. *Appl. energy*, **105**, 207-216.

Alexander, B., Mitchell, R., Gür, T. 2012. Experimental and modeling study of biomass conversion in a solid carbon fuel cell. *J. Electrochem. Soc.*, **159**(3), B347-B354.

Angın, D., Altintig, E., Köse, T.E. 2013. Influence of process parameters on the surface and chemical properties of activated carbon obtained from biochar by chemical activation. *Bioresour. Technol.*, **148**, 542-549.

599 Appels, L., Baeyens, J., Degrève, J., Dewil, R. 2008. Principles and potential of the anaerobic
600 digestion of waste-activated sludge. *Prog. Energy Combust. Sci.*, **34**(6), 755-781.
601 Barisano, D., Freda, C., Nanna, F., Fanelli, E., Villone, A. 2012. Biomass gasification and in-bed
602 contaminants removal: Performance of iron enriched Olivine and bauxite in a process of
603 steam/O_2 gasification. *Bioresour. Technol.*, **118**, 187-194.
604 Bazargan, A., Kostić, M.D., Stamenković, O.S., Veljković, V.B., McKay, G. 2015. A calcium
605 oxide-based catalyst derived from palm kernel shell gasification residues for biodiesel
606 production. *Fuel*, **150**, 519-525.
607 Bazargan, A., Rough, S.L., McKay, G. 2014. Compaction of palm kernel shell biochar for
608 application as solid fuel. *Biomass Bioenerg.*, **70**, 489-497.
609 Beesley, L., Moreno-Jiménez, E., Gomez-Eyles, J.L., Harris, E., Robinson, B., Sizmur, T. 2011.
610 A review of biochar' potential role in the remediation, revegetation and restoration of
611 contaminated soils. *Environ. Pollut.*, **159**(12), 3269-3282.
612 Bhandari, P.N., Kumar, A., Bellmer, D.D., Huhnke, R.L. 2014. Synthesis and evaluation of
613 biochar-derived catalysts for removal of toluene (model tar) from biomass-generated producer
614 gas. *Renew. Energy*, **66**, 346-353.
615 Brewer, C.E., Schmidt-Rohr, K., Satrio, J.A., Brown, R.C. 2009. Characterization of biochar
616 from fast pyrolysis and gasification systems. *Environ. Prog. Sustain. Energy*, **28**(3), 386-396.
617 Brewer, C.E., Unger, R., Schmidt-Rohr, K., Brown, R.C. 2011. Criteria to select biochar for field
618 studies based on biochar chemical properties. *Bioenergy Res.*, **4**(4), 312-323.
619 Brewer, C.E., Chuang, V.J., Masiello, C.A., Gonnermann, H., Gao, X., Dugan, B., Driver, L.E.,
620 Panzacchi, P., Zygourakis, K., Davies, C.A. 2014. New approaches to measuring biochar
621 density and porosity. *Biomass Bioenerg.*, **66**, 176-185.

622 Carpenter, D.L., Bain, R.L., Davis, R.E., Dutta, A., Feik, C.J., Gaston, K.R., Jablonski, W.,
623 Phillips, S.D., Nimlos, M.R. 2010. Pilot-scale gasification of corn stover, switchgrass, wheat
624 straw, and wood: 1. Parametric study and comparison with literature. *Ind. Eng. Chem. Res.*,
625 **49**(4), 1859-1871.
626 Cetin, E., Moghtaderi, B., Gupta, R., Wall, T. 2004. Influence of pyrolysis conditions on the
627 structure and gasification reactivity of biomass chars. *Fuel*, **83**(16), 2139-2150.
628 Chan, F.L., Tanksale, A. 2014. Review of recent developments in Ni-based catalysts for biomass
629 gasification. *Renew. Sustainable Energy Rev.*, **38**, 428-438.
630 Cheah, S., Malone, S.C., Feik, C.J. 2014. Speciation of sulfur in biochar produced from pyrolysis
631 and gasification of oak and corn stover. *Environ. Sci. Technol.*, **48**(15), 8474-8480.
632 Chen, H., Liu, D., Shen, Z., Bao, B., Zhao, S., Wu, L. 2015. Functional biomass carbons with
633 hierarchical porous structure for supercapacitor electrode materials. *Electrochim. Acta*, **180**,
634 241-251.
635 Deal, C., Brewer, C.E., Brown, R.C., Okure, M.A., Amoding, A. 2012. Comparison of kiln-
636 derived and gasifier-derived biochar as soil amendments in the humid tropics. *Biomass*
637 *Bioenerg.*, **37**, 161-168.
638 Dehkhoda, A.M., West, A.H., Ellis, N. 2010. Biochar based solid acid catalyst for biodiesel
639 production. *Appl. Catal. A.*, **382**(2), 197-204.
640 Ducousso, M., Weiss-Hortala, E., Nzihou, A., Castaldi, M.J. 2015. Reactivity enhancement of
641 gasification biochar for catalytic applications. *Fuel*, **159**, 491-499.
642 Dupont, C., Nocquet, T., Da Costa, J.A., Verne-Tournon, C. 2011. Kinetic modelling of steam
643 gasification of various woody biomass chars: influence of inorganic elements. *Bioresour.*
644 *Technol.*, **102**(20), 9743-9748.

645 El-Rub, Z.A., Bramer, E., Brem, G. 2008. Experimental comparison of biomass chars with other
646 catalysts for tar reduction. *Fuel*, **87**(10), 2243-2252.
647 Elleuch, A., Halouani, K., Li, Y. 2015. Investigation of chemical and electrochemical reactions
648 mechanisms in a direct carbon fuel cell using olive wood charcoal as sustainable fuel. *J. Power*
649 *Sources*, **281**, 350-361.
650 Elmouwahidi, A., Zapata-Benabithe, Z., Carrasco-Marín, F., Moreno-Castilla, C. 2012.
651 Activated carbons from KOH-activation of argan (Argania spinosa) seed shells as
652 supercapacitor electrodes. *Bioresour. Technol.*, **111**, 185-190.
653 Enders, A., Hanley, K., Whitman, T., Joseph, S., Lehmann, J. 2012. Characterization of biochar
654 to evaluate recalcitrance and agronomic performance. *Bioresour. Technol.*, **114**, 644-653.
655 Esfahani, R.A.M., Osmieri, L., Specchia, S., Yusup, S., Tavasoli, A., Zamaniyan, A. 2017. H_2-
656 rich syngas production through mixed residual biomass and HDPE waste via integrated
657 catalytic gasification and tar cracking plus bio-char upgrading. *Chem. Eng. J.*, **308**, 578-587.
658 Fortier, H., Westreich, P., Selig, S., Zelenietz, C., Dahn, J. 2008. Ammonia, cyclohexane,
659 nitrogen and water adsorption capacities of an activated carbon impregnated with increasing
660 amounts of $ZnCl_2$, and designed to chemisorb gaseous NH_3 from an air stream. *J. Colloid*
661 *Interface Sci.*, **320**(2), 423-435.
662 Gabhi, R.S., Kirk, D.W., Jia, C.Q. 2017. Preliminary investigation of electrical conductivity of
663 monolithic biochar. *Carbon*, **116**, 435-442.
664 Giddey, S., Badwal, S., Kulkarni, A., Munnings, C. 2012. A comprehensive review of direct
665 carbon fuel cell technology. *Prog. Energy Combust. Sci.*, **38**(3), 360-399.

666 Griffith, S.M., Banowetz, G.M., Gady, D. 2013. Chemical characterization of chars developed
667 from thermochemical treatment of Kentucky bluegrass seed screenings. *Chemosphere*, **92**(10),
668 1275-1279.
669 Guan, G., Chen, G., Kasai, Y., Lim, E.W.C., Hao, X., Kaewpanha, M., Abuliti, A., Fushimi, C.,
670 Tsutsumi, A. 2012. Catalytic steam reforming of biomass tar over iron-or nickel-based catalyst
671 supported on calcined scallop shell. *Appl. Catal. B.*, **115**, 159-168.
672 Hammond, J., Shackley, S., Sohi, S., Brownsort, P. 2011. Prospective life cycle carbon
673 abatement for pyrolysis biochar systems in the UK. *Energy Policy*, **39**(5), 2646-2655.
674 Han, J., Kim, H. 2008. The reduction and control technology of tar during biomass
675 gasification/pyrolysis: An overview. *Renew. Sustainable Energy Rev.*, **12**(2), 397-416.
676 Hansen, V., Hauggaard-Nielsen, H., Petersen, C.T., Mikkelsen, T.N., Müller-Stöver, D. 2016a.
677 Effects of gasification biochar on plant-available water capacity and plant growth in two
678 contrasting soil types. *Soil Tillage Res.*, **161**, 1-9.
679 Hansen, V., Müller-Stöver, D., Ahrenfeldt, J., Holm, J.K., Henriksen, U.B., Hauggaard-Nielsen,
680 H. 2015. Gasification biochar as a valuable by-product for carbon sequestration and soil
681 amendment. *Biomass Bioenerg.*, **72**, 300-308.
682 Hansen, V., Müller-Stöver, D., Munkholm, L.J., Peltre, C., Hauggaard-Nielsen, H., Jensen, L.S.
683 2016b. The effect of straw and wood gasification biochar on carbon sequestration, selected soil
684 fertility indicators and functional groups in soil: An incubation study. *Geoderma*, **269**, 99-107.
685 Hardy, B., Dufey, J. 2017. The resistance of centennial soil charcoal to the "Walkley-Black"
686 oxidation. *Geoderma*, **303**, 37-43.
687 Hernández, J.J., Lapuerta, M., Monedero, E. 2016. Characterisation of residual char from
688 biomass gasification: effect of the gasifier operating conditions. *J. Clean. Prod.*, **138**, 83-93.

689 Huggins, T.M., Pietron, J.J., Wang, H., Ren, Z.J., Biffinger, J.C. 2015. Graphitic biochar as a
690 cathode electrocatalyst support for microbial fuel cells. *Bioresour. Technol.*, **195**, 147-153.
691 Ibarrola, R., Shackley, S., Hammond, J. 2012. Pyrolysis biochar systems for recovering
692 biodegradable materials: A life cycle carbon assessment. *Waste Manage.*, **32**(5), 859-868.
693 Jung, J.-M., Lee, J., Choi, D., Oh, J.-I., Lee, S.-R., Kim, J.-K., Kwon, E.E. 2017. Biochar as
694 porous media for thermally-induced non-catalytic transesterification to synthesize fatty acid
695 ethyl esters from coconut oil. *Energy Convers. Manage.*, **145**, 308-313.
696 Kasozi, G.N., Zimmerman, A.R., Nkedi-Kizza, P., Gao, B. 2010. Catechol and humic acid
697 sorption onto a range of laboratory-produced black carbons (biochar). *Environ. Sci. Technol.*,
698 **44**(16), 6189-6195.
699 Kastner, J.R., Miller, J., Geller, D.P., Locklin, J., Keith, L.H., Johnson, T. 2012. Catalytic
700 esterification of fatty acids using solid acid catalysts generated from biochar and activated
701 carbon. *Catal. Today*, **190**(1), 122-132.
702 Kim, M., Lee, Y., Park, J., Ryu, C., Ohm, T.-I. 2016. Partial oxidation of sewage sludge
703 briquettes in a updraft fixed bed. *Waste Manage.*, **49**, 204-211.
704 Klinghoffer, N.B., Castaldi, M.J., Nzihou, A. 2012. Catalyst properties and catalytic performance
705 of char from biomass gasification. *Ind. Eng. Chem. Res.*, **51**(40), 13113-13122.
706 Le, C., Kolaczkowski, S. 2015. Steam gasification of a refuse derived char: reactivity and
707 kinetics. *Chem. Eng. Res. Des.*, **102**, 389-398.
708 Lee, J., Jung, J.-M., Oh, J.-I., Ok, Y.S., Kwon, E.E. 2017. Establishing a Green Platform for
709 Biodiesel Synthesis via Strategic Utilization of Biochar and Dimethyl Carbonate. *Bioresour.*
710 *Technol.*, In Press.

711 Lehmann, J., Rillig, M.C., Thies, J., Masiello, C.A., Hockaday, W.C., Crowley, D. 2011. Biochar
712 effects on soil biota-a review. *Soil Biol. Biochem.*, **43**(9), 1812-1836.
713 Leijenhorst, E., Assink, D., Van de Beld, L., Weiland, F., Wiinikka, H., Carlsson, P., Öhrman, O.
714 2015. Entrained flow gasification of straw-and wood-derived pyrolysis oil in a pressurized
715 oxygen blown gasifier. *Biomass Bioenerg.*, **79**, 166-176.
716 Li, X., Liu, L., Wang, X., Ok, Y.S., Elliott, J.A., Chang, S.X., Chung, H.-J. 2017. Flexible and
717 Self-Healing Aqueous Supercapacitors for Low Temperature Applications: Polyampholyte Gel
718 Electrolytes with Biochar Electrodes. *Sci. Rep.*, **7**.
719 Li, X., Shen, Q., Zhang, D., Mei, X., Ran, W., Xu, Y., Yu, G. 2013. Functional groups determine
720 biochar properties (pH and EC) as studied by two-dimensional ^{13}C NMR correlation
721 spectroscopy. *PloS One*, **8**(6), e65949.
722 Li, X., Zhu, Z., Chen, J., De Marco, R., Dicks, A., Bradley, J., Lu, G. 2009. Surface modification
723 of carbon fuels for direct carbon fuel cells. *J. Power Sources*, **186**(1), 1-9.
724 Liu, H., Luo, C., Kato, S., Uemiya, S., Kaneko, M., Kojima, T. 2006. Kinetics of CO_2/Char
725 gasification at elevated temperatures: Part I: Experimental results. *Fuel Process. Technol.*,
726 **87**(9), 775-781.
727 Loha, C., Gu, S., De Wilde, J., Mahanta, P., Chatterjee, P.K. 2014. Advances in mathematical
728 modeling of fluidized bed gasification. *Renew. Sustainable Energy Rev.*, **40**, 688-715.
729 Luo, C., Lü, F., Shao, L., He, P. 2015. Application of eco-compatible biochar in anaerobic
730 digestion to relieve acid stress and promote the selective colonization of functional microbes.
731 *Water Res.*, **68**, 710-718.

732 Ma, Z., Xiao, R., Zhang, H. 2016. Catalytic steam reforming of bio-oil model compounds for
733 hydrogen-rich gas production using bio-char as catalyst. *Int. J. Hydrogen Energy*, **42**(6), 3579-
734 3585
735 Maneerung, T., Liew, J., Dai, Y., Kawi, S., Chong, C., Wang, C.-H. 2016. Activated carbon
736 derived from carbon residue from biomass gasification and its application for dye adsorption:
737 kinetics, isotherms and thermodynamic studies. *Bioresour. Technol.*, **200**, 350-359.
738 Manyà, J.J. 2012. Pyrolysis for biochar purposes: a review to establish current knowledge gaps
739 and research needs. *Environ. Sci. Technol.*, **46**(15), 7939-7954.
740 Marks, E.A., Mattana, S., Alcañiz, J.M., Pérez-Herrero, E., Domene, X. 2016. Gasifier biochar
741 effects on nutrient availability, organic matter mineralization, and soil fauna activity in a multi-
742 year Mediterranean trial. *Agric. Ecosyst. Environ.*, **215**, 30-39.
743 McBeath, A.V., Smernik, R.J., Schneider, M.P., Schmidt, M.W., Plant, E.L. 2011. Determination
744 of the aromaticity and the degree of aromatic condensation of a thermosequence of wood
745 charcoal using NMR. *Org. Geochem.*, **42**(10), 1194-1202.
746 Mermoud, F., Golfier, F., Salvador, S., Van de Steene, L., Dirion, J.-L. 2006. Experimental and
747 numerical study of steam gasification of a single charcoal particle. *Combust. Flame*, **145**(1),
748 59-79.
749 Meyer, S., Glaser, B., Quicker, P. 2011. Technical, economical, and climate-related aspects of
750 biochar production technologies: A literature review. *Environ. Sci. Technol.*, **45**(22), 9473-
751 9483.
752 Mohan, D., Sarswat, A., Ok, Y.S., Pittman, C.U. 2014. Organic and inorganic contaminants
753 removal from water with biochar, a renewable, low cost and sustainable adsorbent-A critical
754 review. *Bioresour. Technol.*, **160**, 191-202.

Munnings, C., Kulkarni, A., Giddey, S., Badwal, S. 2014. Biomass to power conversion in a direct carbon fuel cell. *Int. J. Hydrogen Energy*, **39**(23), 12377-12385.

Naisse, C., Alexis, M., Plante, A., Wiedner, K., Glaser, B., Pozzi, A., Carcaillet, C., Criscuoli, I., Rumpel, C. 2013. Can biochar and hydrochar stability be assessed with chemical methods? *Org. Geochem.*, **60**, 40-44.

Nguyen, T.L.T., Hermansen, J.E., Nielsen, R.G. 2013. Environmental assessment of gasification technology for biomass conversion to energy in comparison with other alternatives: the case of wheat straw. *J. Clean. Prod.*, **53**, 138-148.

Nzihou, A., Stanmore, B., Sharrock, P. 2013. A review of catalysts for the gasification of biomass char, with some reference to coal. *Energy*, **58**, 305-317.

Ojeda, G., Mattana, S., Àvila, A., Alcañiz, J.M., Volkmann, M., Bachmann, J. 2015. Are soil-water functions affected by biochar application? *Geoderma*, **249**, 1-11.

Pacioni, T.R., Soares, D., Di Domenico, M., Rosa, M.F., Moreira, R.d.F.P.M., José, H.J. 2016. Bio-syngas production from agro-industrial biomass residues by steam gasification. *Waste Manage.*, **58**, 221-229.

Pereira, E.I.P., Suddick, E.C., Six, J. 2016. Carbon abatement and emissions associated with the gasification of walnut shells for bioenergy and biochar production. *PloS One*, **11**(3), e0150837.

Peterson, S.C., Jackson, M.A. 2014. Simplifying pyrolysis: Using gasification to produce corn stover and wheat straw biochar for sorptive and horticultural media. *Ind. Crops Prod.*, **53**, 228-235.

Plácido, J., Capareda, S. 2015. Production of silicon compounds and fulvic acids from cotton wastes biochar using chemical depolymerization. *Ind. Crops Prod.*, **67**, 270-280.

777 Prasara-A, J., Gheewala, S.H. 2016. Sustainable utilization of rice husk ash from power plants: A
778 review. *J. Clean. Prod.*.
779 Qian, K., Kumar, A. 2015. Reforming of lignin-derived tars over char-based catalyst using Py-
780 GC/MS. *Fuel*, **162**, 47-54.
781 Qian, K., Kumar, A., Zhang, H., Bellmer, D., Huhnke, R. 2015. Recent advances in utilization of
782 biochar. *Renew. Sustainable Energy Rev.*, **42**, 1055-1064.
783 Rabou, L.P., Zwart, R.W., Vreugdenhil, B.J., Bos, L. 2009. Tar in biomass producer gas, the
784 Energy research Centre of the Netherlands (ECN) experience: an enduring challenge. *Energy*
785 *Fuels*, **23**(12), 6189-6198.
786 Rafatullah, M., Sulaiman, O., Hashim, R., Ahmad, A. 2010. Adsorption of methylene blue on
787 low-cost adsorbents: a review. *J. Hazard. Mater.*, **177**(1), 70-80.
788 Rogovska, N., Laird, D., Cruse, R., Trabue, S., Heaton, E. 2012. Germination tests for assessing
789 biochar quality. *J. Environ. Qual.*, **41**(4), 1014-1022.
790 Rollinson, A.N. 2016. Gasification reactor engineering approach to understanding the formation
791 of biochar properties. *Proc. R. Soc. A.*, **472**, 20150841.
792 Scala, F., Chirone, R., Salatino, P. 2006. Combustion and attrition of biomass chars in a fluidized
793 bed. *Energy Fuels*, **20**(1), 91-102.
794 Shackley, S., Carter, S., Knowles, T., Middelink, E., Haefele, S., Haszeldine, S. 2012a.
795 Sustainable gasification-biochar systems? A case-study of rice-husk gasification in Cambodia,
796 Part II: Field trial results, carbon abatement, economic assessment and conclusions. *Energy*
797 *Policy*, **41**, 618-623.
798 Shackley, S., Carter, S., Knowles, T., Middelink, E., Haefele, S., Sohi, S., Cross, A., Haszeldine,
799 S. 2012b. Sustainable gasification-biochar systems? A case-study of rice-husk gasification in

800 Cambodia, Part I: Context, chemical properties, environmental and health and safety issues.
801 *Energy Policy*, **42**, 49-58.
802 Shafeeyan, M.S., Daud, W.M.A.W., Houshmand, A., Shamiri, A. 2010. A review on surface
803 modification of activated carbon for carbon dioxide adsorption. *J. Anal. Appl. Pyrolysis*, **89**(2),
804 143-151.
805 Shen, Y. 2015. Chars as carbonaceous adsorbents/catalysts for tar elimination during biomass
806 pyrolysis or gasification. *Renew. Sustainable Energy Rev.*, **43**, 281-295.
807 Shen, Y., Linville, J.L., Ignacio-de Leon, P.A.A., Schoene, R.P., Urgun-Demirtas, M. 2016.
808 Towards a sustainable paradigm of waste-to-energy process: Enhanced anaerobic digestion of
809 sludge with woody biochar. *J. Clean. Prod.*, **135**, 1054-1064.
810 Shen, Y., Yoshikawa, K. 2013. Recent progresses in catalytic tar elimination during biomass
811 gasification or pyrolysis-A review. *Renew. Sustainable Energy Rev.*, **21**, 371-392.
812 Sohi, S., Krull, E., Lopez-Capel, E., Bol, R. 2010. A review of biochar and its use and function
813 in soil. *Adv. Agron.*, **105**, 47-82.
814 Spokas, K.A. 2010. Review of the stability of biochar in soils: predictability of O: C molar ratios.
815 *Carbon Manag.*, **1**(2), 289-303.
816 Spokas, K.A., Novak, J.M., Stewart, C.E., Cantrell, K.B., Uchimiya, M., DuSaire, M.G., Ro, K.S.
817 2011. Qualitative analysis of volatile organic compounds on biochar. *Chemosphere*, **85**(5),
818 869-882.
819 Sun, H., Hockaday, W.C., Masiello, C.A., Zygourakis, K. 2012. Multiple controls on the
820 chemical and physical structure of biochar. *Ind. Eng. Chem. Res.*, **51**(9), 3587-3597.
821 Taupe, N., Lynch, D., Wnetrzak, R., Kwapinska, M., Kwapinski, W., Leahy, J. 2016. Updraft
822 gasification of poultry litter at farm-scale-A case study. *Waste Manage.*, **50**, 324-333.

823 Tay, T., Ucar, S., Karagöz, S. 2009. Preparation and characterization of activated carbon from
824 waste biomass. *J. Hazard. Mater.*, **165**(1), 481-485.
825 Thompson, K.A., Shimabuku, K.K., Kearns, J.P., Knappe, D.R., Summers, R.S., Cook, S.M.
826 2016. Environmental comparison of biochar and activated carbon for tertiary wastewater
827 treatment. *Environ. Sci. Technol.*, **50**(20), 11253-11262.
828 Thompson, S.P., Parker, J.E., Tang, C.C. 2014. Thermal breakdown of calcium carbonate and
829 constraints on its use as a biomarker. *Icarus*, **229**, 1-10.
830 Wang, B., Li, C., Liang, H. 2013. Bioleaching of heavy metal from woody biochar using
831 Acidithiobacillus ferrooxidans and activation for adsorption. *Bioresour. Technol.*, **146**, 803-806.
832 Wiedemeier, D.B., Abiven, S., Hockaday, W.C., Keiluweit, M., Kleber, M., Masiello, C.A.,
833 McBeath, A.V., Nico, P.S., Pyle, L.A., Schneider, M.P. 2015. Aromaticity and degree of
834 aromatic condensation of char. *Org. Geochem.*, **78**, 135-143.
835 Wiedner, K., Rumpel, C., Steiner, C., Pozzi, A., Maas, R., Glaser, B. 2013. Chemical evaluation
836 of chars produced by thermochemical conversion (gasification, pyrolysis and hydrothermal
837 carbonization) of agro-industrial biomass on a commercial scale. *Biomass Bioenerg.*, **59**, 264-
838 278.
839 Wu, H., Yip, K., Tian, F., Xie, Z., Li, C.-Z. 2009. Evolution of char structure during the steam
840 gasification of biochar produced from the pyrolysis of various mallee biomass components. *Ind.*
841 *Eng. Chem. Res.*, **48**(23), 10431-10438.
842 Xiao, G., Ni, M.-J., Chi, Y., Cen, K.-F. 2008. Low-temperature gasification of waste tire in a
843 fluidized bed. *Energy Convers. Manage.*, **49**(8), 2078-2082.
844 Xiu, S., Shahbazi, A., Li, R. 2017. Characterization, Modification and Application of Biochar for
845 Energy Storage and Catalysis: A Review. *Trends in Renewable Energy*, **3**(1), 86-101.

Xu, C.C., Hamilton, S., Ghosh, M. 2009. Hydro-treatment of Athabasca vacuum tower bottoms in supercritical toluene with microporous activated carbons and metal-carbon composite. *Fuel*, **88**(11), 2097-2105.

Xue, Y., Gao, B., Yao, Y., Inyang, M., Zhang, M., Zimmerman, A.R., Ro, K.S. 2012. Hydrogen peroxide modification enhances the ability of biochar (hydrochar) produced from hydrothermal carbonization of peanut hull to remove aqueous heavy metals: batch and column tests. *Chem. Eng. J.*, **200**, 673-680.

Yargicoglu, E.N., Sadasivam, B.Y., Reddy, K.R., Spokas, K. 2015. Physical and chemical characterization of waste wood derived biochar. *Waste Manage.*, **36**, 256-268.

Yeo, T., Tan, I., Abdullah, M. 2012. Development of adsorption air-conditioning technology using modified activated carbon-A review. *Renew. Sustainable Energy Rev.*, **16**(5), 3355-3363.

Yip, K., Tian, F., Hayashi, J.-i., Wu, H. 2009. Effect of alkali and alkaline earth metallic species on biochar reactivity and syngas compositions during steam gasification. *Energy Fuels*, **24**(1), 173-181.

Yu, M.M., Masnadi, M.S., Grace, J.R., Bi, X.T., Lim, C.J., Li, Y. 2015. Co-gasification of biosolids with biomass: Thermogravimetric analysis and pilot scale study in a bubbling fluidized bed reactor. *Bioresour. Technol.*, **175**, 51-58.

Yu, X.-Y., Ying, G.-G., Kookana, R.S. 2009. Reduced plant uptake of pesticides with biochar additions to soil. *Chemosphere*, **76**(5), 665-671.

Zhang, X., Zhang, S., Yang, H., Feng, Y., Chen, Y., Wang, X., Chen, H. 2014. Nitrogen enriched biochar modified by high temperature CO_2-ammonia treatment: Characterization and adsorption of CO_2. *Chem. Eng. J.*, **257**, 20-27.

868 Zhao, P., Mao, Z., Jin, D., Zhao, P., Sun, B., Sun, W., Pang, X. 2015. Investigation on log
869 responses of bulk density and thermal neutrons in coalbed with different ranks. *J. Geophys.*
870 *Eng.*, **12**(3), 477.

Figure
Click here to download Figure: Figure.docx

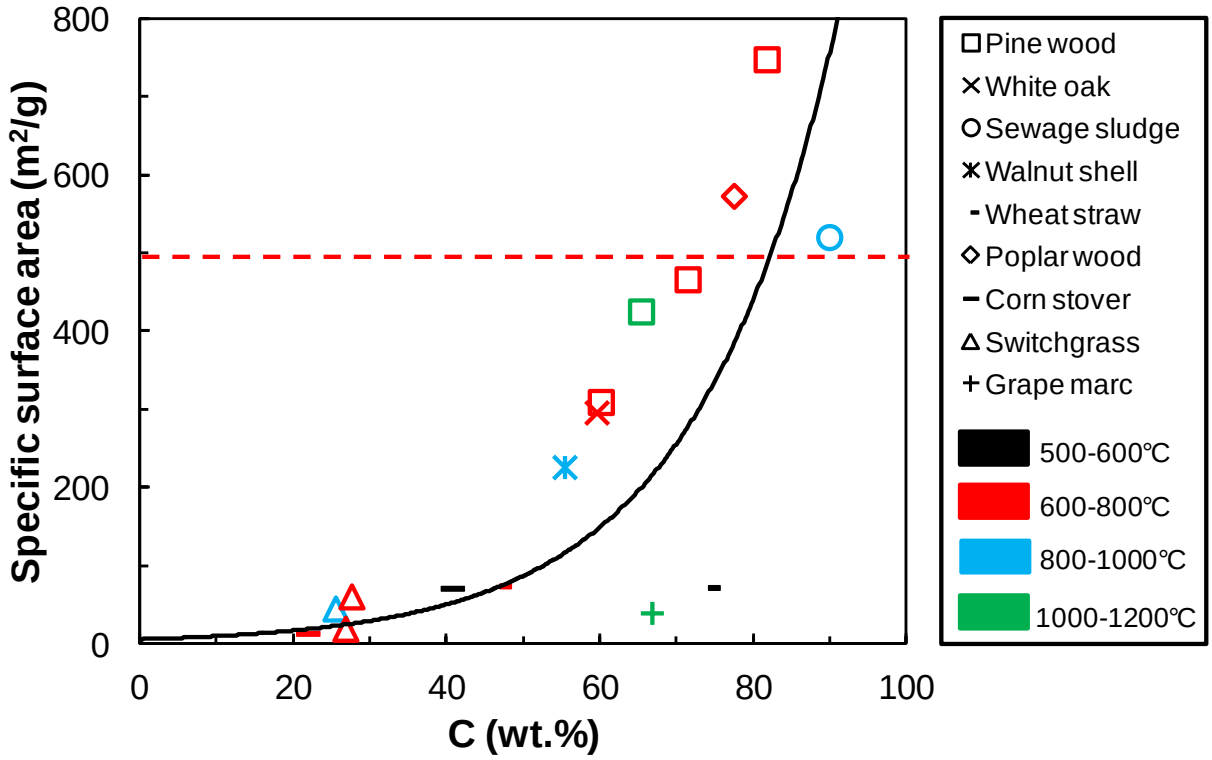

Fig. 1. Specific surface areas and total carbon content in gasification biochar (Brewer et al., 2011; Ducousso et al., 2015; Hansen et al., 2016a; Hansen et al., 2015; Hansen et al., 2016b; Kim et al., 2016; Pereira et al., 2016; Peterson & Jackson, 2014; Rollinson, 2016; Shen et al., 2016). The solid line denotes the exponential fit. The mid-point or average value is used if a range or multiple values is (are) given by an original study. The red dash line denotes the lower bound of the specific surface area of activated carbon (500 m^2 g^{-1}) (Yeo et al., 2012).

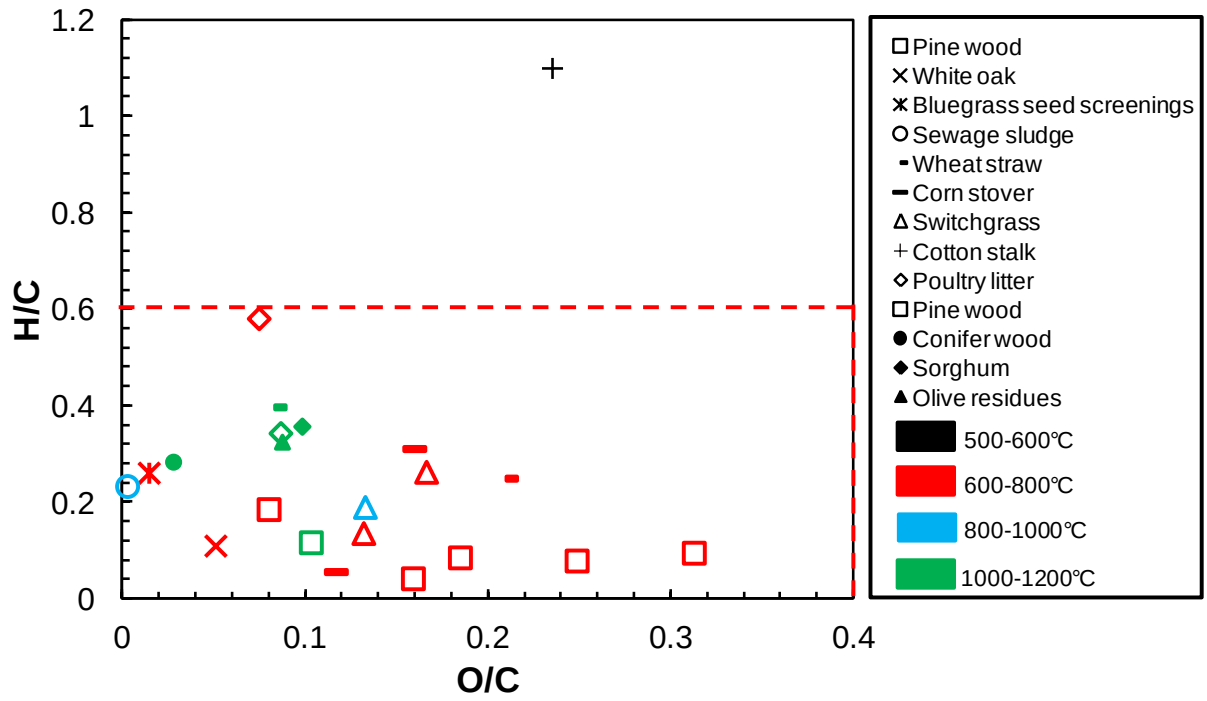

Fig. 2. Van Krevelen diagram for gasification biochar. Data is from existing studies (Brewer et al., 2011; Ducousso et al., 2015; Griffith et al., 2013; Hansen et al., 2016a; Hansen et al., 2015; Hansen et al., 2016b; Kim et al., 2016; Marks et al., 2016; Ojeda et al., 2015; Plácido & Capareda, 2015; Rollinson, 2016; Shen et al., 2016; Taupe et al., 2016; Wiedner et al., 2013). The red dash lines denote the recommended upper bound limits (0.6 and 0.4, respectively) of H/C and O/C ratios for biochar materials by EBC.

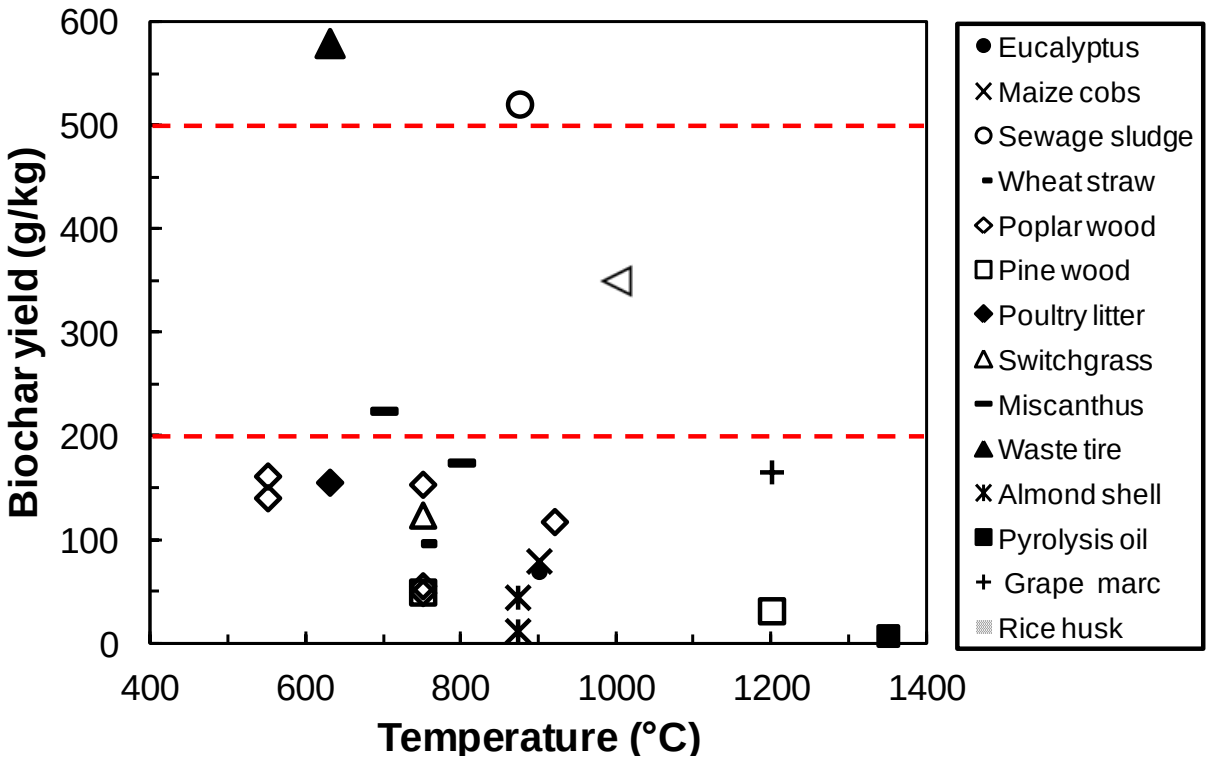

Fig. 3. Gasification biochar yields with respect to temperature, the types of gasifiers and feedstocks, and gasifying agents reported by previous studies (Barisano et al., 2012; Deal et al., 2012; Hansen et al., 2016a; Hansen et al., 2015; Hansen et al., 2016b; Hernández et al., 2016; Kim et al., 2016; Klinghoffer et al., 2012; Leijenhorst et al., 2015; Ojeda et al., 2015; Shackley et al., 2012b; Taupe et al., 2016). The mid-point or average value is used if a range or multiple values is (are) given by an original study. The red dash lines denote the biochar yield of pyrolysis (Manyà, 2012).

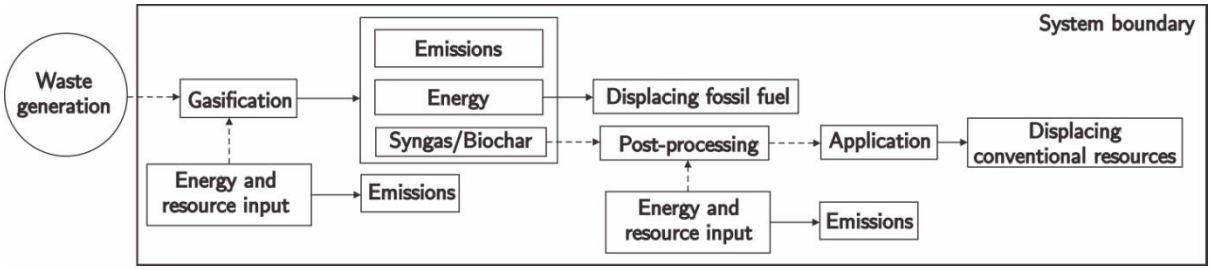

Fig. 4. The system boundary of LCA for a gasification-based waste disposal scheme.

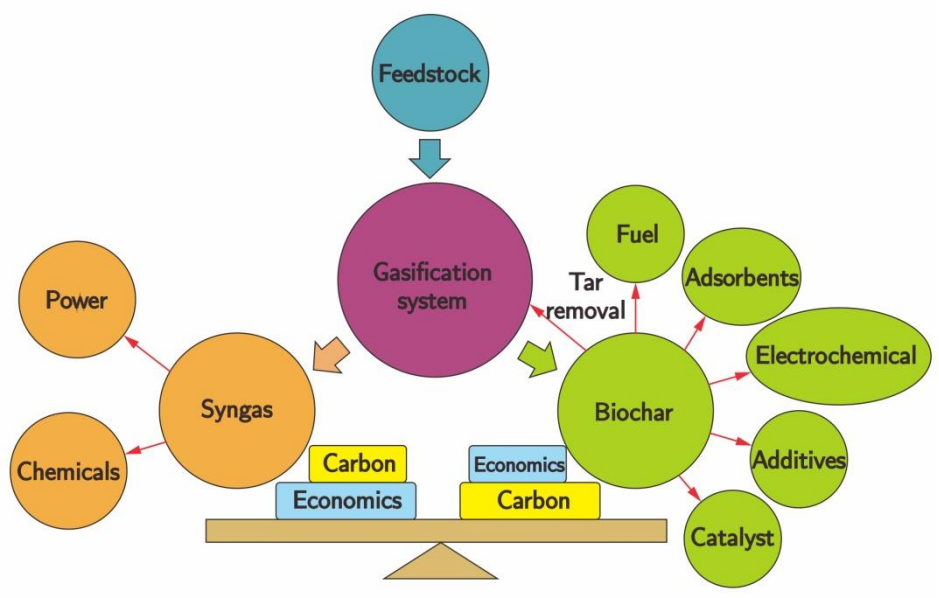

Fig. 5. The overall balance between syngas and biochar production for an economically and environmentally feasible gasification system.

Table

Table 1. A summary of gasification conditions (gasifier types, temperature, and gasifying agent), total carbon, ash, and inorganic elements in gasification biochars

Feedstock	Gasifier types	Temperature (°C)	Gasifying agent	Ash (wt. %)	C (wt. %)	Inorganic elements (mg/g)	References
Pine wood	Fluidized bed	600 – 710[#]	Steam and or N_2	18.69	60.04	SiO_2 (73.15), Al_2O_3 (3.2), TiO_2 (0.03), Fe_2O_3 (12.54), CaO (3.30), MgO (83.38), Na_2O (0.17), K_2O (2.36), P_2O_5 (0.99), SO_3 (0.09), Cl (0.02), CO_2 (1.96)	Shen et al. (2016)
White oak	Fluidized bed	600 – 710[#]	Steam and or N_2	34.90	59.49	SiO_2 (141.33), Al_2O_3 (5.97), TiO_2 (0.07), Fe_2O_3 (23.55), CaO (7.94), MgO (149.99), Na_2O (0.17), K_2O (0.20), P_2O_5 (0.44), SO_3 (0.42), Cl (0.03), CO_2 (4.37)	Shen et al. (2016)
Kentucky bluegrass seed mill screenings	Updraft	600 -650	Air	46.3	45.7	NH_4-N (0.0149), NO_3-N (1.081), Incubation-N (0.0248), Mineralizable-N (0.0099), K (48.203), Ca (13.580), P (11.680), Mg (5.702), S (3.879), Cl (2.268), Fe (1.031), Mn (0.703), B (0.0272), Na (0.275), Zn (0.0895), Cu (0.0251), Al (0.869)	Griffith et al. (2013)
Switchgrass	Downdraft	N. A.	N. A.	N. A.	64.80	P (0.27), Ca (2.81), K (0.73), Mg (0.45), Na (0.13), Fe (0.29), Zn (97.8)[†], Cu (8.8)[†], Mn (394.5)[†], Ni (4.6)[†], Al (1408.0)[†]	Bhandari et al. (2014)
Switchgrass	Fluidized bed	N. A.	N. A.	N. A.	1.38	P (0.04), Ca (0.13), K (0.17), Mg (2.65), Na (0.03), Fe (0.78), Zn (79.4)[†], Cu (5.7)[†], Mn (130.1)[†], Ni (303.7)[†], Al (426.0)[†]	Bhandari et al. (2014)
Sewage sludge	Updraft	800 - 950	Air	73.17[§]	89.85	Si (180), Al (63.7), P (53.3), Fe (41.9), K (20.6), Ca (4.89), Mg (11.1), Na (10.1), Mn (2.4), Zn (0.863), Cu (1.21), Cr (0.27), Pb (0.0617), Ni (0.237), Zr (0.0766)	Kim et al. (2016)
Corn stover	Fluidized	850	Steam	47.1	42.0	Fe (10)[†], Ca (14), Mg (9.2)[†], K (54) Si (14)	Cheah et al. (2014)
Winter wheat straw	Fluidized	750	Air	N. A.	46.8	K (72), Na (2.6)	Hansen et al. (2016a), Hansen et al. (2015), Hansen et al. (2016b)
Pine wood	Downdraft	1200	Steam	N. A.	65.29	K (19), Na (2.0)	Hansen et al. (2016a), Hansen et al. (2015), Hansen et al. (2016b)
Pine wood	N. A.	600 - 900	N. A.	10.79	79.34	P (1.337), Na (0.48), K (9.36), Ca (20.52), Mg (2.1), Cu (0.012), Co (0.008), Cr (0.034), Ni (0.025), Pb (0.016), Zn (0.256), As (9×10^{-4}), Cd (1.38×10^{-3}), Sb (4.35×10^{-4}), $CaCO_3$ (33.4), C-CO_3 (4)	Marks et al. (2016)

Rice husk	Downdraft	900 - 1100	N. A.	63	35	Al (0.092-0.543), Ba (0.019-0.048), B (0.00181-0.00538), Ca (0.609-1.94), Cu (0.0082-0.0153), Fe (0.066-0.107), Mg (0.162-0.658), Mn (0.135-0.47), K (0.595-2.418), Si (0.066-0.199), Na (0.076-0.65), Sr (0.00187-0.0091), Ti (0.00179-0.00525), Zn (0.0117-0.0442)	Shackley et al. (2012b)
Pine wood	Fluidized	600-900	Air	N. A.	71	Ca (92.3), K (8.3), Na (0.8), P (0.8), Fe (0.08), Cd (1.2), Cr (26.0), Cu (224), Ni (10), Pb (9.1), Zn (982-1504)	Ojeda et al. (2015)
Pine wood	Updraft	1000	Air	N. A.	N. A.	Al (0.35×10^{-3}), Ca (12×10^{-3}), Co (0), K (2.0×10^{-3}), Mg (0.11×10^{-3}), Mn (0.02×10^{-3}), Na (0.18×10^{-3}), P (0.06×10^{-3}), Sc (0.02×10^{-3}), Si (2.31×10^{-3}), Ti (0.18×10^{-3}), Zn (0.07×10^{-3})	Huggins et al. (2015)
Poultry litter	Updraft	580 - 680	Air	54.8	33.1	P (29.3), K (87.8), Na (10.4), Ca (44.1), Cl (1.2), Mg (18.3), Fe (2.389), Mn (1.577), Zn (1.229), Cu (0.273), B (0.148), Al (1.121), Pb (0.87), Cd (1.03), Ni (21.6), Cr (16.1)	Taupe et al. (2016)

Values are estimated based on the study by Carpenter et al. (2010).
† The unit is ppm.
§ The values are on a dry basis.